Characterisation of DNA damage induced by near infrared multi-photon absorption

E L Leatherbarrow, J V Harper, P O'Neill

MRC Radiation and Genome Stability Unit, Harwell, Didcot, Oxon., OX11 0RD, UK

S W Botchway, M Dillingham, A W Parker

Central Laser Facility, CCLRC Rutherford Appleton Laboratory, Chilton, Didcot, Oxon., OX11 0QX, UK

Main contact email address: *p.oneill@har.mrc.ac.uk*

Introduction

When cells are exposed to radiation serious cellular lesions are introduced into the DNA. These include random double strand breaks (DSB), single strand breaks (SSB), base damage and clustered damage sites, a specific feature of radiation induced DNA damage. It is known that DNA bases absorb maximally in the UVC wavelength range (200-290nm), resulting in the formation of bulky lesions and complex DNA DSB sites. This complex damage has long been thought to be a critical determinant leading to loss of genome stability[1,2]. It has previously been shown using 254nm UV excitation that DSB are formed in cells in the presence of BrdU, an intercalator dye and laser scissors[3]. Previously we reported the induction of DNA double strand breaks in cells exposed to a near infrared (NIR) ultrashort pulse laser through multi-photon processes in the presence of Hoechst dye but absence of integrated BrdU (Leatherbarrow *et al.*, CLF Annual Report 2003-2004).

Recently, the substantial phosphorylation of the histone H2AX has been identified as an early step in the response of cells to DSB[4,5,6] and has been adopted as a beacon of DSB formation in cells. This response has now been used to investigate DSB formation following low LET radiation in a number of studies[4,7,8]. Several other proteins involved in the sensing, signalling and repair of DSB have now been identified and are known to co-localise with γ-H2AX following DNA DSB induction in mammalian cells. The phosphatidylinositol 3-kinases, DNA-PK (DNA-dependent protein kinase), ATM (ataxia telangiectasia mutated) and ATR (ATM and Rad3-related) have all been implicated in the phosphorylation of H2AX[9], although ATM is the major kinase involved in the phosphorylation of H2AX following ionising radiation. In the absence of ATM DNA-PK, rather than ATR, is responsible for low levels of phosphorylation[10,11]. p53 Binding Protein 1 or 53BP1 has been shown to rapidly localise to sites of DNA DSB[12]. 53BP1 may indeed be responsible for the activation of ATM following ionizing radiation as the phosphorylation of ATM substrates has been shown to be suppressed in cells with diminished 53BP1[13,14,15]. Although, it appears that H2AX phosphorylation is required for the formation of 53BP1 foci at sites of DNA DSB[16,17]. RAD51, which forms filaments along the unwound DNA strand to facilitate strand invasion[18,19], is an integral protein of the homologous recombination DNA damage repair pathway dominant in late S early G2 of the mammalian cell cycle and has been shown to co-localise with DNA damage signalling and repair proteins such as γ-H2AX[5].

The mechanisms of DNA damage repair have been extensively studied either *in vitro* using ionising radiation or more recently with microbeam technology. Although the use of a microbeam provides a method to investigate DNA damage within single cells, the dimension of the microbeam produced is still very large (several microns). This results in a large amount of damage being induced throughout the cell along the track of the beam. This may in turn saturate the DNA damage sensing, signalling and repair pathways of interest in this study. Recently we developed a NIR laser microbeam methodology to investigate single cell DNA damage dynamics. Unlike multi-photonic excitation, where the wavelength of the photon must match an electronic absorption band of the molecule under study, multi-photon processes occur when a molecule interacts with two or more photons that sum to provide an equivalent quanta of energy to create the electronic excited state or, as in some cases, a photonionised species. For instance, three photons absorbed by a molecule in a stepwise fashion from a 750 nm laser source is equivalent in energy to absorption of a single photon of 250nm. In this method the NIR irradiation induces DNA damage in individual mammalian cells through multi-photon processes. There are several advantages of this technique over the other methods. Mammalian cells are transparent to the NIR light. Therefore the damage will only be induced at the confocal point, in a single z-plane within the cell nucleus, where the multi-photon absorption occurs (Figure 1A). Since the multi-photon processes only occurs within the 3D submicron femtolitre volume, any damage is localised within such dimensions unlike conventional ionising radiation, where damage can be formed along the length of the particle track, or UV radiation, where majority of cell components absorb (Figure 1B). Interpretation of the damage data is not complicated by damage to other cellular components outside the actual 3D region of interest.

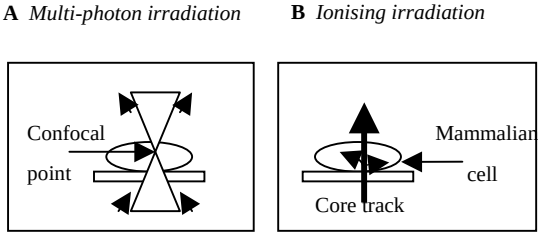

Figure 1. Schematic of irradiation of a mammalian cell by multi-photon processes (A) and α-particles (B). It can be seen that multi-photon irradiation will only cause damage within a single z-plane at the confocal point, whereas ionising irradiation will induce damage throughout the cell along the core track.

We now report some preliminary findings on the induction and subsequent repair of DNA DSB induced in mammalian cells by multi-photon NIR irradiation following raster scanning and pin-pointing individual locations within single cells by computer controlled ability to targeting and revisiting these locations for laser spotting.

Methods

Cell Lines

Chinese hamster V79-4 and *xrs*-5 cells and human fibroblast HF19 cells were maintained with twice weekly subculture in minimal essential medium (MEM) supplemented with 10 % foetal calf serum (FCS), 100 μg/ml penicillin streptomycin and 2 mM L-glutamine. They were grown at 37ºC in the presence of 5 % CO_2.

Experimental set up

The 'laser microbeam' was generated using a titanium sapphire laser (Ti:Sa, Tsunami, Spectra Physics laser, Germany) operating at 700-850 nm, 110 fs pulse width with an output power of 1.2 W. This was used to pump an optical parametric oscillator to generate visible output, 550 – 640 nm laser light with similar characteristic as the Ti:Sa laser. A 20 W argon ion laser (Spectra Physics laser, Germany) was used to pump the Ti:Sa system. The laser beams were expanded and reflected

into the back of an inverted microscope (Nikon TE2000). Also attached to the microscope is a Q-Cam 10 bit colour camera for wide field imaging and a BioRad MRC 600 confocal scanning unit for the fluorescence imaging. Irradiations and imaging were carried out using either a x40 (na 0.95) or x60 oil (na 1.4) objective. The microscope was fitted with a computer controlled microscope stage (Marhauzer, Germany).

Raster Scanning

A computer software system was developed in-house to allow the cells to be irradiated by raster scanning using a femtosecond pulsed Tsuanami Titanium:Sapphire (Ti:S) laser. Predefined raster scan steps, 12μm steps in and a raster scan area of 0.25cm x 0.5cm in the present study, were selected prior to the initiation of laser scanning.

Laser Spotting

A computer software system was developed in-house to allow irradiation of cells at specific coordinates which can be re-visited following processing by immunofluorescence techniques. Individual cells were located on a live cell image and irradiation coordinates pre-selected and logged. A shutter was opened and closed for the duration of the irradiation through computer controlled software. Conditions of the irradiation were optimised for laser power, distance between targeted locations, laser wavelength and cell culture conditions.

Immunofluorescence

Irradiation was carried out at 10^{o}C (optimum temperature defined in previous studies-REF); following irradiation the cold medium was removed and replaced with medium warmed to 37°C and the cells were placed into an incubator (37°C) for the stated repair times. Cells were then rinsed with 1x PBS and fixed with 3% paraformaldehyde for 30 min. Cells were rinsed in 1x PBS, placed in 1% triton X-100 for 10 min, blocked in 1% bovine serum albumin and 1% fish skin gelatin for 1 h and incubated at 4°C overnight with the primary antibody diluted 1:200 in the blocking medium. The cells were rinsed, blocked for 1 h and incubated with a conjugated secondary antibody for 1 h. Cells were rinsed and mounted with vectashield (Vector), an antifade medium. When the cells are fixed the cell thickness is reduced to ~3μm.

Image capturing

A 2.5 μm thick z-plane slice through the centre of each fixed cell was captured using a BioRad MRC 600 confocal microscope with 488nm (FITC) or 633nm (Cy5) excitation, a x60 oil objective and an optimised and unchanging gain setting following raster scanning of the cells. The resolution of the z-phase slice of ~2.5 μm is as a consequence of the low level of emitted light thereby requiring the confocal pinhole to be opened wide. Images of the fluorescence from the cells in the field of view were obtained by rastering through the x,y plane. The single z plane 1μm thick slices were analysed for foci formation. The number of foci within each cell is not dependent upon whether one or two z-series images were obtained, the latter representing data for the whole thickness of a given cell.

Following laser spotting the cells were returned to the computer controlled motorised microscope stage and the exact irradiation coordinated recalled to observe the outcome of the specific irradiated position. Fluorescence imaging was carried out using a BioRad MRC600 scan head attached to the microscope or BioRad Radiance attached to an Olympus microscope.

Antibodies

The rabbit anti-phospho-H2AX polyclonal, mouse anti-phospho-H2AX monoclonal and mouse anti-phospho-ATM antibodies were purchased from Upstate Cell Signalling Solutions. The anti-53BP1 antibody was purchased from Bethyl Laboratories. The anti-αRAD51 antibody was purchased from Calbiochem. The FITC-conjugated and Cy5-conjugated secondary antibodies were purchased from Jackson Immuno.

Results

Identification of defined sites in the cell and revisiting the co-ordinates for micro-irradiation of cells.

We tested the computer controlled system to establish the ability to induce DNA DSB, detected as γ-H2AX foci, in DSB repair deficient hamster xrs-5 cells, and the formation of 53BP1 foci (recruited to DSB) in DSB repair proficient hamster V79-4 cells at pre-defined co-ordinates within cell nuclei and the accuracy of focal irradiation at the sites recorded are shown in Figure 2.

The pre-defined and selected co-ordinates are also shown as an irradiation map or cell image at the time of irradiation. The areas of DNA damage, as indicated by foci formation, match the pre-selected co-ordinates demonstrating the flexibility of the NIR multi-photon irradiation method used in these studies for investigation of DNA damage induction and repair when inducing damage at multiple defined locations within a cell or several cells.

Sensing, Signalling and Repair of induced DNA DSB

In our previous studies, we used the γ-H2AX assay to detect DNA DSB induced in mammalian cells exposed to multi-photon NIR radiation. From optimisation of experiments with cells containing BrdU incorporated into the DNA in the presence or absence of Hoechst dye, the greatest level of detectable DNA damage, as measured by γ-H2AX foci, is in the presence of Hoechst dye but in the absence of BrdU. These conditions were therefore used in the present study.

During this session, we set out to investigate the formation of foci of proteins involved in the sensing, signalling and repair of DNA DSB. DSB repair proficient V79-4 cells and human HF19 cells, and repair deficient hamster xrs-5 cells were exposed to a NIR multi-photon laser at a wavelength of 730nm either by raster scanning of the cells or by irradiation at pre-defined co-ordinates within the nucleus of the cell (see above).

The cells, which were raster scanned with the laser, were investigated for both foci formation of the proteins of interest and the potential co-localisation of these proteins at sites of damage over the course of time. From preliminary time dependent studies using immuno-histochemical detection of proteins, γ–H2AX, ATM, 53BP1 and RAD51 proteins were all found to produce foci in the 3 cell lines tested at various times but with different time profiles after irradiation. ATM (a phosphatidylinositol 3-kinases involved in DSB signalling) was found to generate foci within ~1min following exposure at the sites of DNA DSB, and was seen to co-localise with γ-H2AX over a defined time course. Figure 3a shows the co-localisation of γ-H2AX and ATM foci at 10 mins post-irradiation. It can be seen, even at this relatively early time point, that ATM foci are beginning to dissipate and γ-H2AX are becoming stronger. By 30 mins post-irradiation ATM foci have disappeared but γ-H2AX foci are still visible 24 hours post-irradiation. γ-H2AX is also a much more amplified response to DNA damage than the formation of ATM foci, with over 2000 H2AX molecules becoming phosphorylated in response to a

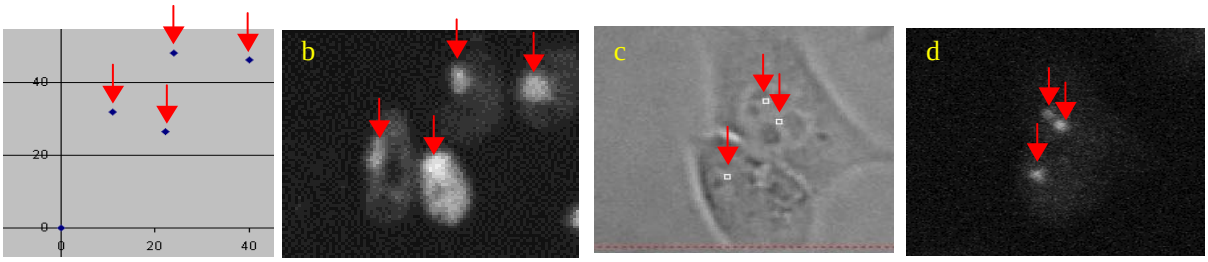

Figure 2. (a) Logged coordinates for the points of irradiation of xrs-5 cells. (b) γ-H2AX foci formed following irradiation of xrs-5 cells with 25 mW Ti:S laser for 5 s; points were located using the re-visiting software. (c) Logged coordinates on the live cell image for the points of irradiation of V79-4 cells. (d) 53BP1 foci formed following irradiation of V79-4 cells with 25 mW Ti:S laser for 5 s; points were located using the re-visiting software.

single DSB and therefore shows as a stronger signal when visualised immuno-histochemically.

Visible foci of 53BP1, although implicated in the activation of ATM following ionising radiation, appeared within 5 min after formation of ATM foci and peak foci formation was observed at 30 min post irradiation. 53PB1 was seen to co-localise with γ-H2AX at sites of DSB at various time points (Figure 3b). RAD51, a central protein involved in the repair of DNA DSB by homologous recombination (HR), was found to form foci at sites of DSB but only in ~50% of the cell population at 60 min post-irradiation (Figure 3c). HR only occurs in cells during the late S and early G2 phases of the cell cycle when a sister chromatid is present to act as a repair template. The percentage of cells showing RAD51 foci correlates with the percentage of cells in S/G2 from FACS analysis on exponentially growing cell (data not shown). The number of cells within the irradiated population showing RAD51 foci increased with time potentially due to cell cycle blocks being initiated in G1 by DSB. Whether the RAD51 foci arise from prompt DSB or through DSB generated at stalled replication forks needs to be investigated. ATM, 53BP1 and RAD51 foci were all seen to co-localise with γ–H2AX foci following raster scanning of V79-4, *xrs*-5 and HF-19 cells at various time points (Typical examples shown in Figures 3a, b and c respectively). The detection of foci by immuno-histochemistry or in real-time with fluorescently tagged proteins needs to be developed further to ensure background, non-specific levels of staining are minimised.

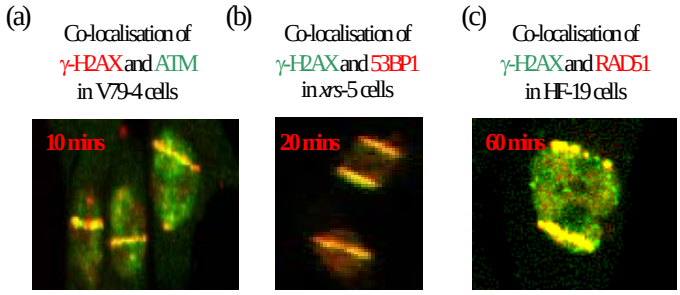

Figure 3. (a) γ-H2AX is shown in red, ATM is shown in green; co-localisation produces a yellow colour. (b) γ-H2AX is shown in green, 53BP1 is shown in red; co-localisation produces a yellow colour. (c) γ-H2AX is shown in green, RAD51 is shown in red; co-localisation produces a yellow colour. The lines indicate the laser scan through the cell.

Conclusions

1) The computer control of the stage has been tested successfully to optimise irradiation within defined locations within cells.

2) We have obtained very preliminary data on the sensing, signalling and repair of DNA DSB induced by NIR multi-photon irradiation over a time course. Of the proteins tested, ATM was seen to be initially recruited promptly at the sites of DSB with subsequent phosphorylation of histone H2AX. 53BP1 was seen to form foci after H2AX phosphorylation and ultimately co-localise with the other sensing and signalling proteins at the sites of damage. RAD51, involved in the HR repair pathway, was seen to co-localise with γ-H2AX foci 30 min post-irradiation demonstrating the co-ordinated handover of damage from signalling to repair pathways. The detected DSBs may have arisen at replication as RAD51 foci are only detected in a percentage of irradiated cells. Studies are currently on-going at MRC to optimise detection of foci (using ionising radiation as the DNA damage inducer) so that further studies will focus on elucidating the kinetics of recruitment of proteins to sites of DNA damage in mammalian cells following exposure to NIR multi-photon irradiation and the role of cell cycle. Fluorescently tagged proteins will allow us to take advantage of the fast time response of the technology to explore processes occurring at early times and to follow the response in real time.

References

1. D T Goodhead,
Int J Radiat Biol 65, 7-17, (1994)

2. J F Ward,
Prog Nucleic Acid Res Mol Biol 35, 95-125, (1988)

3. C L Limoli, E Giedzinski, W M Bonner, J E Cleaver,
Proc Natl Acad Sci U S A 99, 233-238, (2002)

4. D R Pilch, O A Sedelnikova, C Redon, A Celeste,
A Nussenzweig, W M Bonner,
Biochem Cell Biol 81, 123-129, (2003)

5. T T Paull, E P Rogakou, V Yamazaki, C U Kirchgessner,
M Gellert, W M Bonner,
Curr Biol 10, 886-895

6. E P Rogakou, C Boon, C Redon, W M Bonner,
(1999) *J Cell Biol* 146, 905-916, (2000)

7. K Rothkamm, I Kruger, L H Thompson, M Lobrich,
Mol Cell Biol 23, 5706-5715, (2003)

8. K Rothkamm, M Lobrich,
Proc Natl Acad Sci U S A 100, 5057-5062, (2003)

9. T Stiff, M O'Driscoll, N Rief, K Iwabuchi, M Lobrich,
P A Jeggo,
Cancer Res 64, 2390-2396, (2004)

10. S Burma, B P Chen, M Murphy, A Kurimasa, D J Chen,
J Biol Chem 276, 42462-42467, (2001)

11. P A Jeggo, M Lobrich,
Cell Cycle 4, 359-362, (2005)

12. L B Schultz, N H Chehab, T D Malikzay, T D Halazonetis,
J Biol Chem 151, 1381-1390, (2000)

13. R A DiTullio, T A Mochan Jr., M Venere, J Bartkova,
M Sehested, J Bartek, T D Halazonetis,
Nat Cell Biol 4, 998-1002, (2002)

14. O Fernandez-Capetillo, H T Chen, A Celeste, I Ward,
P J Romanienko, J C Morales, K Naka, Z Xia,
R D Camerini-Otero, N Motoyama, P B Carpenter,
W M Bonner, J Chen, A Nussenzweig,
Nat Cell Biol 4, 993-997, (2002)

15. B Wang, S Matsuoka, P B Carpenter, S J Elledge,
Science 298, 1435-1438, (2002)

16. I M Ward, K Minn, J van Deursen, J Chen,
Mol Cell Biol 23, 2556-2563, (2003)

17. I M Ward, K Minn, K G Jorda, J Chen,
J Biol Chem 278, 19579-19582, (2003)

18. P Baumann, F E Benson, and S C West,
Cell 87, 757-766, (1996)

19. P Baumann, S C West,
Trends Biochem Sci 23, 247-251, (1998)